Astron. Astrophys. 335, 1029–1039 (1998)

ASTRONOMY
AND
ASTROPHYSICS

A bipolar outflow in the M 1-67 nebula around the Wolf-Rayet star WR 124⋆

Marco Sirianni[1,2], **Antonella Nota**[1,⋆⋆], **Anna Pasquali**[1], **and Mark Clampin**[1]

[1] Space Telescope Science Institute, 3700 San Martin Drive, Baltimore, MD 21218, USA
[2] Center of Studies and Activities for Space "G. Colombo", University of Padova, Italy

Received 1 September 1997 / Accepted 13 November 1997

Abstract. Ground based high resolution coronographic images of the inner M 1-67 nebula ($\simeq 40'' \times 60''$) around the Wolf Rayet WR 124 have been obtained with the Johns Hopkins Adaptive Optic Coronograph at the Swope 40″ telescope, Las Campanas, in the light of Hα + [NII]. The inner M 1-67 nebula appears very clumpy and remarkably axisymmetric. In addition, we present new high signal-to-noise long slit spectroscopic data, with full spatial coverage of the nebula ($\simeq 90'' \times 75''$), which have been used the save derive its radial velocity map (from the [NII] 6583 Å line profile). The radial velocity data reveal the presence of two different motions in the enviroment of WR 124: a spherical hollow shell, 46″ in radius, expanding with a velocity of 46 km s^{-1}, and a newly discovered bipolar outflow, with a velocity of 88 km s^{-1}. Their dynamical ages are estimated to be 2×10^4 yrs and 1.2×10^4 yrs respectively, and their overall N enriched composition seem to indicate that they formed during the post-main sequence evolution of WR 124. This scenario is consistent with two subsequent outbursts, possibly occurred during a previous LBV phase.

Key words: stars: individual: WR 124 – ISM: individual objects: M 1–67 – stars: mass-loss – stars: Wolf-Rayet – ISM: bubbles – ISM: jets and outflows

1. Introduction

M 1-67 is a bright, clumpy nebula surrounding the star WR 124, a Population I WN8 star characterized by a very high velocity of 200 km s^{-1} (Bertola 1964) and often called *Merrill's star*. The nebula shows a clumpy and irregular distribution of gas which is mostly condensated in bright knots and filaments.

The classification of the M 1-67 nebula has been subject of debate in the past years. Although first classified as a H II region (Sharpless 1959), the fact that both the central star and the nebula are moving at high heliocentric velocity ($\sim$200 km s^{-1}) prompted its inclusion in the catalog of planetary nebulae (Bertola 1964; Perek & Kohoutek 1967; Pişmiş & Recillas-Cruz 1979). Later on, IR and radio investigation (Cohen & Barlow 1975) suggested it was a ring nebula around a Wolf-Rayet star and M 1-67 was therefore removed from the planetary nebulae catalog (Kohoutek 1978). Nevertheless, such a classification was later suggested again by van der Hucht et al. (1985).

Recently, detailed abundance analysis of the nebula (Esteban et al. 1991, 1993) revealed N enhancement and O deficiency typical of material ejected from the star in a previous – maybe LBV – phase, and pointed to a progenitor more massive than those usually associated to planetary nebulae central stars: M 1-67 was finally classified as an *ejected type* nebula. At the same time, a second indipendent result ruling out a planetary nebula status was derived by its distance determination. In order for M 1-67 to be a planetary nebula, its distance should have been in the range between 0.46 Kpc (van der Hucht et al. 1985) and 0.9 Kpc (Bertola 1964). However, the interstellar Na I D_2 absorption spectrum of WR 124 shows a velocity consistent with the gas velocity dispersion expected from the galactic rotation at a distance of 4-5 Kpc (Crawford & Barlow 1991). A similar large distance of 4.33 Kpc was also obtained by Cohen & Barlow (1975), and by Pişmiş & Recillas-Cruz (1979) [4.5 kpc].

The nebular spectra of M 1-67 display very strong Hα and [NII] lines, with an intensity ratio I(Hα)/I([NII]λ 6583)= 1 - 1.2 (Barker 1978; Solf & Carsenty 1982). [OII] $\lambda\lambda$3726, 3729 are detected while [OIII] $\lambda\lambda$4959, 5007 and [OI] $\lambda\lambda$6300, 6364 are almost completely absent (Barker 1978). Investigations of the physical conditions of M 1-67 suggest a very low ionization level (Bertola 1964), with an electron temperature T_e ranging between 6200$\pm$500 K (Esteban et al. 1991) and 7500 K (Barker 1978), and an electron density n_e between 200 and 1000 cm^{-3} (Solf & Carsenty 1982; Esteban et al. 1991). The chemical composition of the nebula (Esteban et al. 1991) shows N enhancement by a factor of 4-7.5 with respect to the galactic abundance gradient for HII regions and O depletion by a factor of 5-7.5, suggesting that O has been processed into N mainly via the ON cycle. Moreover, Esteban et al. (1991) estimated an upper limit of 0.2 for the ratio between the mass of swept-up interstellar gas to the mass ejected by the central star, implying that M 1-67 is almost completely composed of stellar material ejected by the central star in a previous evolutionary phase, and no relevant mixing with the local interstellar medium has occurred.

Send offprint requests to: A. Nota

⋆ Based on observations obtained at the European Southern Observatory, La Silla

⋆⋆ Affiliated with the Astrophysics Division, Space Science Department of the European Space Agency

The dynamics of the nebula are still subject of debate: from Fabry-Perot interferometry in Hα, Pişmiş & Recillas-Cruz (1979) found several components in the velocity field of the nebula and proposed anisotropic mass loss from active spots located on opposite emispheres of the star along a diameter inclined with respect to the rotation axis. Later, employing a similar technique with improved resolution, Chu & Treffers (1981) found two main velocity components: a narrow component concentrated near the central star at V = 185 km s^{-1} and a broader, more extended, component at V = 150 km s^{-1}. The authors, therefore, argued that these velocity components were probably due to separate "outbursts" experienced by the star in different epochs (about 10^4 to 10^5 yr ago), and that the ejected material had been slowed down and displaced by the interaction with the interstellar medium.

A subsequent high resolution long slit spectroscopical investigation (Solf & Carsenty 1982, thereafter SC) showed a clear splitting in the nebular lines (e.g. [N II] λ6583) with a maximum separation of 92 km s^{-1}. SC derived an overall spherical symmetric velocity field and explained their results invoking the presence of a thin wind-blown expanding shell, probably produced by the interaction of the strong stellar wind with pre-existing material lost by the star in a previous evolutionary phase. These results seemed at variance with the morphology of the inner nebula as showed in previous coronographic imaging by Nota et al. (1995a). Due to the high contrast achieved by the coronograph in the nebular inner regions by occulting the central star, the authors clearly detected the axisymmetric structure of M 1-67. The nebula is clumpy and the clumps seem to be concentrated in two cones originating from the star. The discrepancy between the coronographic images and the dynamics derived by SC has led us to investigate more carefully the kinematical properties of the nebula.

2. The observations

2.1. The images

We have observed M 1-67 with the Johns Hopkins University (JHU) Adaptive Optics Coronograph (AOC) (Clampin et al. 1991) at the Swope 40″ telescope (Las Campanas, Chile), on the night of June 19, 1990. The AOC employs a tip/tilt mirror to compensate for image motion due to atmospheric turbolence and telescope jitter, resulting in improved angular resolution and enhanced contrast. The coronograph has an occulting mask followed by a lens which reimages the telescope exit pupil, where an apodizing mask suppresses diffracted light from the telescope optics. Images were taken in the light of Hα+[NII] (λ = 6560Å, $\Delta\lambda$ = 110Å). The field of view is 42″ × 63″, with a plate scale of 0.22″ pixel^{-1}. A circular occulting mask of 5″ in diameter was used to block the light from WR 124. Although it is not possible to measure the actual seeing in the M 1-67 frames, due to the absence of point sources in the imaged field of view, the prevailing seeing conditions (corrected for image motion) for this set of observations were of the order of 0.8″.

2.2. The spectra

We performed long slit spectroscopy of M 1-67 in May 1995 with EMMI (ESO Multi Mode Instrument), at the ESO 3.5m NTT, La Silla. EMMI was used in the REMD configuration (REd grating spectroscopy at Medium Dispersion) with grating # 6 to achieve a spectral resolution of 0.31 Å pixel^{-1} (at 6563 Å) in the spectral range 6240 - 6880 Å. The effective spectral resolution of this configuration is 1 Å, measured from the FWHM of the lines in the comparison spectra. In Table 1 we present the detailed journal of the spectroscopic observations.

A slit of 1″ × 180″ (with a spatial scale of 0.27″ pixel^{-1}) was used to take medium resolution spectra of all the clumps we had previously identified in the images. In total, we took spectra at 13 positions in the nebula, corresponding to the individual clumps detected in the coronographic image, with exposure times of 1200s per pointing. We took an additional spectrum on the central star with an exposure time of 300s. An additional moderate resolution spectrum was taken in correspondence to one of the brightest clumps (M), with grism # 7, in the range 5080 - 6425 Å, with the objective to detect the [NII] 5755Å line.

We estimate the accuracy of the telescope pointing to be better than 1″. The standard star Ge48-90 was also observed with the same configuration to provide the flux calibration. A number of comparison spectra with an Argon lamp had been acquired interleaved with the different exposures in order to provide accurate wavelength calibration and minimize possible shifts due to changes in telescope position.

2.3. The data reduction

Both images and spectra were reduced using standard IRAF procedures. Each frame was bias subtracted and flat fielded, cleaned from bad columns and cosmic rays. In the images, it was necessary to mask the image of the occulting bar. This was done by setting the value of pixels in this region of the image to zero.

After the basic reduction, the long slit spectra were background subtracted. The sky background was modelled in each frame by using a Chebyshev function of low order. The surface producing the best fit was then used for the subtraction. The spectra were then calibrated in wavelength using the comparison spectra obtained with an Argon lamp. Each scientific frame was wavelength calibrated using an average of the comparison spectra taken immediately before and after the observation. Since the main objective of this work was to determine the nebular radial velocities, we did not apply the extinction correction to the spectral data, nor we flux calibrated them.

3. The results

3.1. The morphology

The inner M 1-67 nebula appears very clumpy and remarkably axisymmetric in the coronographic images ($\simeq$ 42″ × 63″, Fig. 1). For the first time it is possible to notice that most of the emission comes from bright clumps of different shape and

size. The smallest clumps, spherical or slightly elongated, have approximate diameters of 0.04 - 0.06 pc (adopting a distance of 4.5 Kpc for WR 124, Pişmiş & Recillas-Cruz 1979), whereas the largest structures, which show no regular shape, can reach 0.2 pc in size. About 10 bright clumps seem to be distributed along a *"preferred axis"* at PA $\sim 30^o$, while $\simeq 7$ bright structures are located along the NS axis. The majority of the clumps is concentrated within two conical regions originating from the star spanning position angles 0^o to 30^o, and 180^o to 210^o. In Table 2 we have listed all the clumps detected in the coronographic images. For each clump we provide identification, position and slit location at which the clump is detected (from Table 1). The overall *bipolar* symmetry is striking and now clearly visible due to the high contrast achieved by the coronograph in the inner region. This prompted us to reinvestigate the kinematics of the nebula, and in particular to perform the full mapping of the individual clumps we identified in the coronographic images, which had been mostly missed by previous investigations (SC, Chu & Treffers 1981).

3.2. The radial velocity map

In order to achieve full spatial coverage of the M 1-67, we have taken long slit spectra at 13 positions in the nebula, roughly coinciding with the brightest clumps detected in the coronographic image. In Fig. 2 we have superposed the slit positions on the M 1-67 image, and labelled them A to U, so that it is possible to visualize the spectroscopic coverage of the nebula. As we will discuss in more detail later on, at each slit position we detected several clumps: we labelled them in Fig. 2 with numbers ranging from 1 to 27. Their positions are listed in Table 2.

In all nebular spectra taken in the range between 6240 and 6880 Å five emission lines are clearly detected: [NII] λ6548, Hα λ6563, [NII] λ6583 and [SII] $\lambda\lambda$6717, 6731. They are extended and display a hollow structure. In Fig. 3 we show an enlargement of the two-dimensional profile of the [NII] 6583Å line for the most representative slit positions. A first inspection of the figure clearly shows that the structure of this nebular line varies as a function of position with respect to the central star. In most cases, a clear splitting of the line is observed, the blue-shifted component being fainter than the red-shifted component. In addition, both line components consist of many bright condensations, reflecting the clumpy pattern which can be recognized in the coronographic images. The spatial line profiles indicate that each slit position typically includes 5 to 12 very bright structures, which appear to be composed by a number of smaller clumps. All the bright structures that we identified in the coronographic image of M 1-67 are clearly visible in the line profiles. We labelled them in both images and spectra, for easy cross identification (see Figs. 2 and 3).

The main goal of our spectroscopic investigation is to map all the bright individual clumps we identified in the coronographic image, in the attempt to solve the question of the kinematical structure of M 1-67 and discern between the anisotropic outflow (Pişmiş & Recillas-Cruz 1979) or the expanding shell (Solf & Carsenty 1982). The problem of determining the radial velocities of the individual clumps in each slit position has been approached using the following procedure: first, for each pointing position (A to U) we extracted the spatial profile of each nebular line by summing 30 columns along the spatial axis and centered on the line. Then, in order to determine the position and extent of all the bright condensations, every peak in the spatial profile above a fixed threshold (S/N=5) was fitted with a single or multiple gaussian. We recorded the peak location and the FWHM of the fitted profiles, representative of the relative position with respect to the star (along the Right Ascension axis) and of the size of the clumps. Using such values we extracted from each two-dimensional spectrum, along the dispersion axis, a one-dimensional spectrum which was summed across as many rows as the value of the spatial FWHM, and centered on the peak relative position (see Fig. 4 for an outline of the procedure). This extraction procedure compensated for any possible variation in the seeing during the spectroscopic observations. This procedure, applied to all the slit positions, yielded 153 one-dimensional spectra of the brightest clumpy structures. Additional 82 spectra were extracted in the diffuse regions of the nebula (by summing over 5 rows) to study the dynamical properties of the underlying diffuse component of the nebula and to compare them with those found for the clumps. In each one-dimensional spectrum we then fitted the five nebular lines detected with single or multiple gaussian profiles, and recorded the wavelength peak position and the FWHM of each component. The five lines produced very similar measurements, but for the purpose of mapping the dynamics of the gas in the nebula, we considered only the [NII] λ6583 line profiles, which were characterised by a higher S/N (ranging between 15 and 150). 437 radial velocities measurements were obtained from the [NII] λ6583 line, which were then corrected to the heliocentric frame of reference.

The spectrum obtained on the central star (slit position H) shows a very broad Hα with a FWHM of 19.5 pixels, corrisponding to a stellar wind velocity of $\sim$ 450 km s^{-1}. From the Hα line we have obtained for WR 124 a heliocentric radial velocity of 195 km s^{-1} in good agreement with the published values (Merrill 1938; Cohen & Barlow 1975; SC).

4. The model

In order to represent the kinematical structure of M 1-67, we have plotted the heliocentric radial velocities from each slit position as a function of the relative position with respect to the star (Fig. 5). The heliocentric radial velocities range between 60 and 210 km s^{-1}.

The radial velocity distribution is reminiscent of an expanding shell. Nevertheless some clear deviations from spherical symmetry are present especially in the eastern region in the lower velocity range and in the western region at the higher velocity range. These distortions suggest the presence of a second motion component, possibly aligned to a preferential axis. The stellar velocity, marked in Fig. 5, falls at the margin of the radial velocity distribution, suggesting that the star has main-

Table 1. Journal of EMMI observations

Slit label	Offset from the star ($''$)		Date	Exposure time (sec)	Wavelength range (Å)
A	25	N	05/22/95	1200	6240 - 6880
B	15.5	N	05/22/95	1200	6240 - 6880
E	14	N	05/23/95	1200	6240 - 6880
F	9	N	05/22/95	1200	6240 - 6880
M	3	N	05/22/95	1200	6240 - 6880
M	3	N	05/22/95	1200	5080 - 6425
H	0		05/22/95	300	6240 - 6880
Q	1.5	S	05/23/95	1200	6240 - 6880
L	3.5	S	05/23/95	1200	6240 - 6880
O	9	S	05/23/95	1200	6240 - 6880
J	10.5	S	05/23/95	1200	6240 - 6880
K	15	S	05/23/95	1200	6240 - 6880
18	S	05/23/95	1200	6240 - 6880	
U	31	S	05/23/95	1200	6240 - 6880

Table 2. Relative positions of the clumps with respect to the central star (α_{2000}=19h 11′ 31″, δ_{2000} +16^o 51′ 32″)

Clump	α ($''$)	δ($''$)	Slit	Clump	α ($''$)	δ($''$)	Slit
1	-6.0	26.0	A	15	-6.0	0.0	HL
2	25.0	21.0	A	16	12.5	- 4.5	Q
3	1.5	15.5	BE	17	-5.0	- 6.0	O
4	11.0	14.0	BE	18	-4.5	- 10.5	JO
5	17.5	15.5	BE	19	0.5	- 6.0	O
6	1.5	10.0	F	20	-0.5	- 10.5	JO
7	8.7	11.0	F	21	11.0	- 9.0	O
8	16.0	6.0	F	22	-8.5	- 16.0	KT
9	-19.0	10.0	F	23	1.5	- 15.0	K
10	-19.0	2.5	HM	24	5.0	-14.0	K
11	3.5	0.0	HMQ	25	-17.5	- 20.5	T
12	19.0	3.0	M	26	-4.5	- 31.0	U
13	-14.5	0.0	LQ	27	16.0	- 31.5	U
14	-11.5	-1.5	HQ				

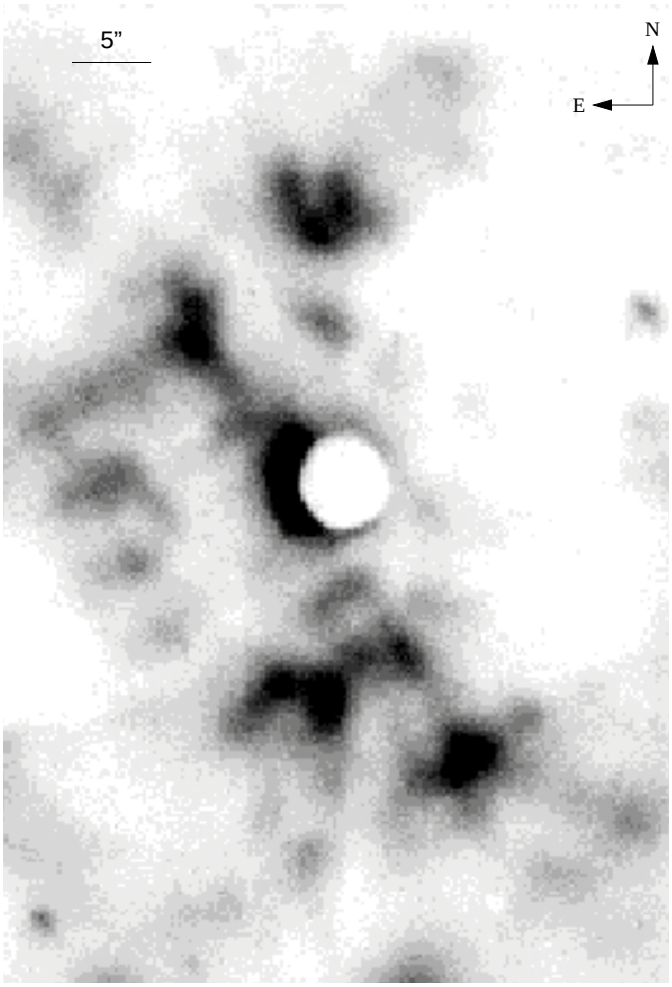

Fig. 1. Coronographic image of the inner M 1-67 nebula taken at the Swope 40″ telescope, Las Campanas (Chile), in the light of Hα+[NII]. The field of view in the image is 42″ × 63″, with a plate scale of 0.22″pixel^{-1}.

tained its fast motion undisturbed, while the entire nebula has significantly slowed down since its original formation.

SC carried out a long-slit spectroscopic study at the 2.2-m telescope of Calar Alto with a spectral resolution of 12 km s^{-1} and a spatial resolution of 2″. With a sample of 150 radial velocities distributed over 80 × 89 ″, they proposed a model in which the emission lines would originate at the surface of a thin spherical shell of angular radius R = 44″, expanding with a velocity V_R = 42 km s^{-1}. The center of expansion was displaced by about 6″ from the position of the central star and had a heliocentric radial velocity V_0 = 158 km s^{-1}, slightly lower than the stellar velocity.

In our analysis, we also have assumed the main component to be an expanding shell. In order to determine the kinematical properties of this structure we have first used the velocity law adopted by SC:

$$(V_{\alpha,\delta} - V_0)^2 = V_R^2[R^2 - (\alpha - \alpha_0)^2 - (\delta - \delta_0)^2]/R^2,$$

where $V_{\alpha,\delta}$ is the heliocentric radial velocity at the position (α, δ) of our sample and (α_0, δ_0) are the spatial coordinates of WR 124. Using the whole sample (437 entries) and a rejection threshold of $\pm$ 15 km s^{-1}, a χ^2 test yielded the following results: 219 sample points ($\simeq$ 50%) belong, within the error of $\pm$ 15 km s^{-1}, to a shell structure of radius R = 46″ expanding with a velocity of V_R = 46 km s^{-1} with respect to a center of expansion moving with a heliocentric radial velocity V_0 = 137 km s^{-1}.

In Fig. 6 (left panel) we have plotted the observed radial velocities, to which we have subtracted the shell expansion center velocity, as function of the position with respect to the star (open squares). We have overlayed in the same figure the radial velocity distribution (filled circles) obtained from the model. We have also plotted (Fig. 6, right panel) the spatial distribution of the points belonging to the expanding shell, superimposed on a large scale image of M 1-67. The overall homogeneous distribution covers almost the entire spatial extent of the nebula. Both the kinematical properties and the size of the shell are in good agreement with the results obtained by SC.

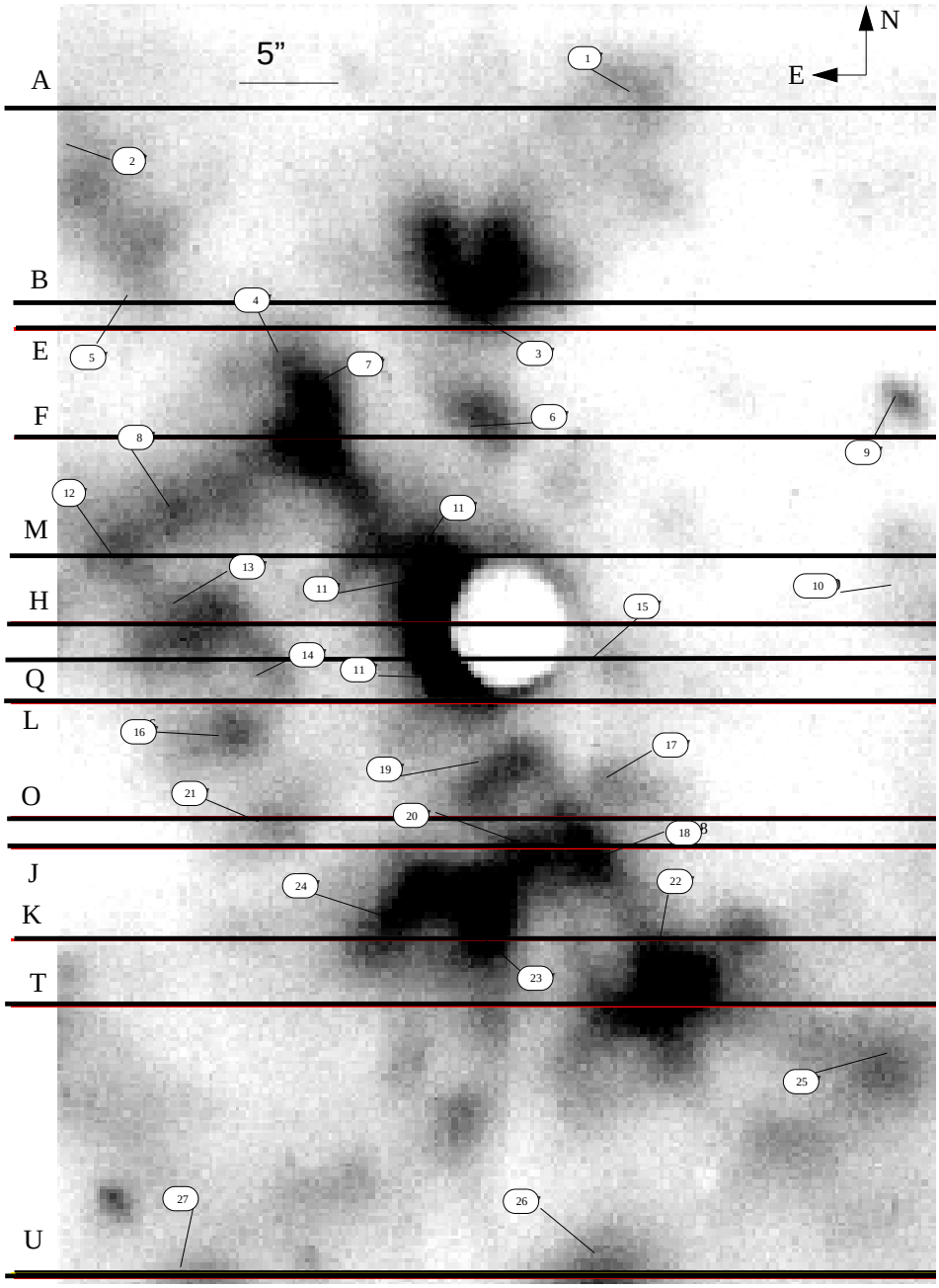

Fig. 2. The slit locations for the spectroscopic observations are here overlayed onto the coronographic image of M 1-67. At each slit position, we identify a number of clumps. We label them with numbers from 1 to 27 (see Table 2 for their relative positions).

We have then subtracted from our total data set all the points belonging to the shell, according to our statistical test. We are left with two structures in the radial velocity diagram (Fig. 7, left panel) which indicate strong departure from spherical symmetry. The large scatter in the data points can be partially explained with a differential impact of the local medium onto the high velocity expanding gas. Nevertheless, two main structures are very clearly identified in the radial velocity diagram. Both structures have an relative radial velocity which, in modulus, is greater than the velocity of the shell; all blueshifted velocities are located to the East of the star, while all the redshifted components are located to the West of the star. The emerging scenario is not of a second expanding shell, but rather of a motion which develops along a bipolar axis. This second motion component joins two regions which are symmetrically located with respect to the shell expansion center. Their location on the projected plane of the sky is shown in Fig. 7 (right panel), and suggests the presence of a bipolar outflow, defined here as motion developing most predominantly along a preferential axis. In this respect, the bipolar outflow represents the best fit to the residual data, when compared to other possibilities such a very elongated ellipsoid, or a second fragmented shell.

The comparison with the image of the nebula allows us to reconstruct the 3-D orientation of the bipolar outflow. For this purpose, it is necessary to determine two angles: first, the inclination of the outflow symmetry axis with respect to the plane

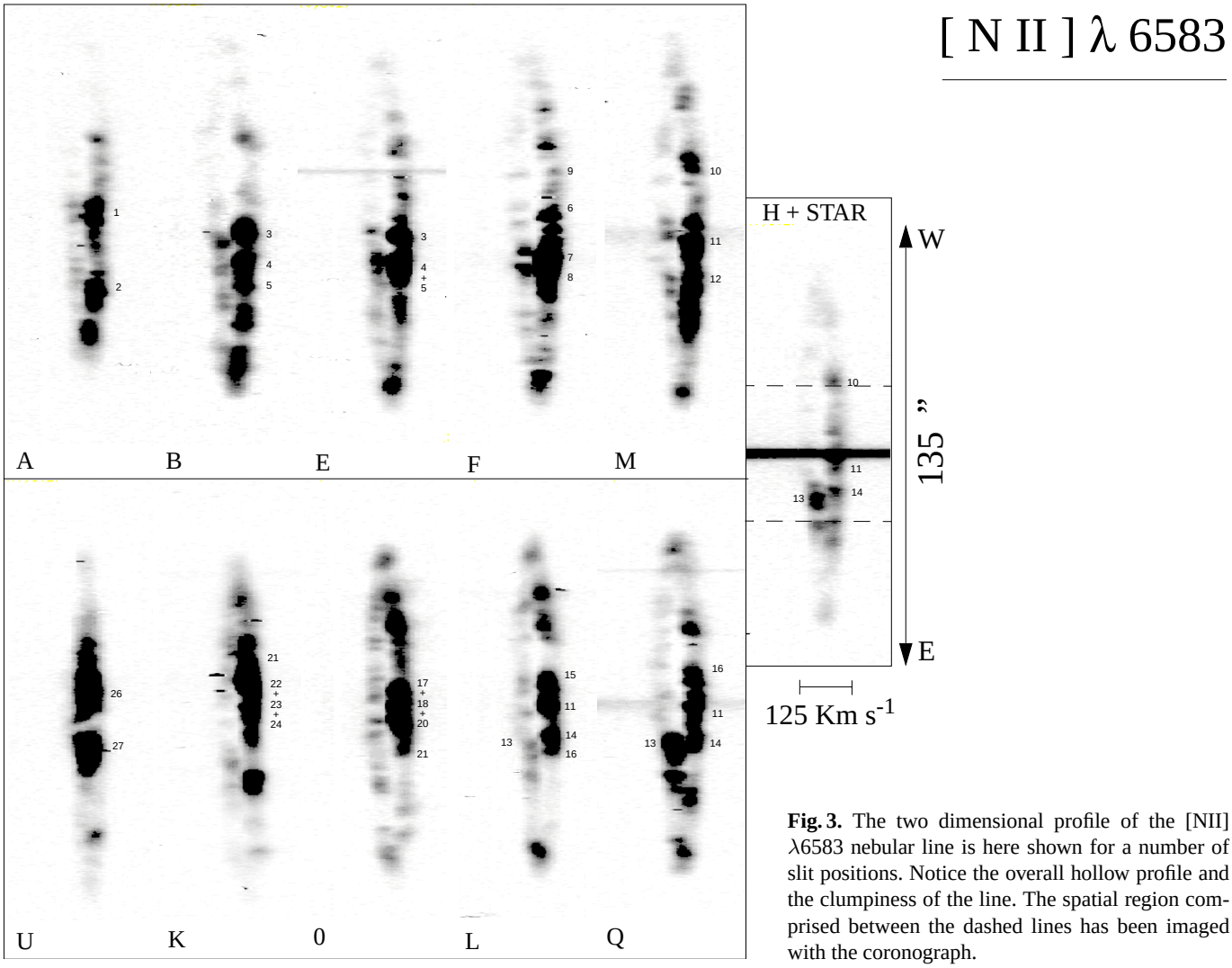

Fig. 3. The two dimensional profile of the [NII] λ6583 nebular line is here shown for a number of slit positions. Notice the overall hollow profile and the clumpiness of the line. The spatial region comprised between the dashed lines has been imaged with the coronograph.

defined by the Line of Sight and the Right Ascension. Second, we need to measure the inclination of such axis with respect to the plane defined by the Line of Sight and Declination. Our 3-D coordinate system is illustrated in Fig. 8, where S is the Line of Sight, α and δ are the Right Ascension and Declination axes, respectively, and r is the symmetry axis of the bipolar outflow. In the figure, θ is the azimuthal angle between r and the S – α plane, θ' is the angle between the projection of r in the α – δ plane (p in the figure) and the α axis, and φ is the inclination angle in the S – α plane and is measured from the α axis.

The three angles are related to each other by the following equations:

$$p^2 = r^2(cos^2\theta cos^2\varphi + sin^2\theta), \quad (1)$$

and

$$tg\theta' = tg\theta/cos\varphi. \quad (2)$$

From the right panel in Fig. 7 we can measure the inclination of the bipolar outflow projected axis p on the α - δ plane, and therefore, the angle θ', which results to be 25^o. We measure a projected dimension (p) of 47″. The distribution of the radial velocities as a function of RA (Fig. 7) gives us also the inclination of the outflow major axis in the S – α plane, that is φ. We measure an angle φ=45^o (Fig. 8d). By introducing the values of θ' and φ in Eq. (2) we obtained the true inclination of the outflow symmetry axis with respect to the line of sight: θ = 18^o. Then from Eq. (1) we derived a real extension r of 48″ for the bipolar structure. For θ = 18^o and $V cos\theta$ = 84 km s^{-1} we have derived a total velocity of V = 88 km s^{-1} for the bipolar outflow.

5. Discussion and conclusions

Our coronographic and spectroscopic investigation reveals two different components in the enviroment of WR 124: a spherical hollow shell, 92″ in diameter expanding at 46 km s^{-1} with respect to a center of expansion moving through space at a heliocentric velocity of 137 km s^{-1}, already detected by SC; and a newly discovered bipolar outflow with a semi dimension of 48″, with a velocity with respect to the shell center of expansion of 88 km s^{-1}. Previous dynamical analyses had proposed either the presence of an anisotropic outflow (Pişmiş & Recillas-Cruz 1979) or a simple expanding shell (SC). Our results show that

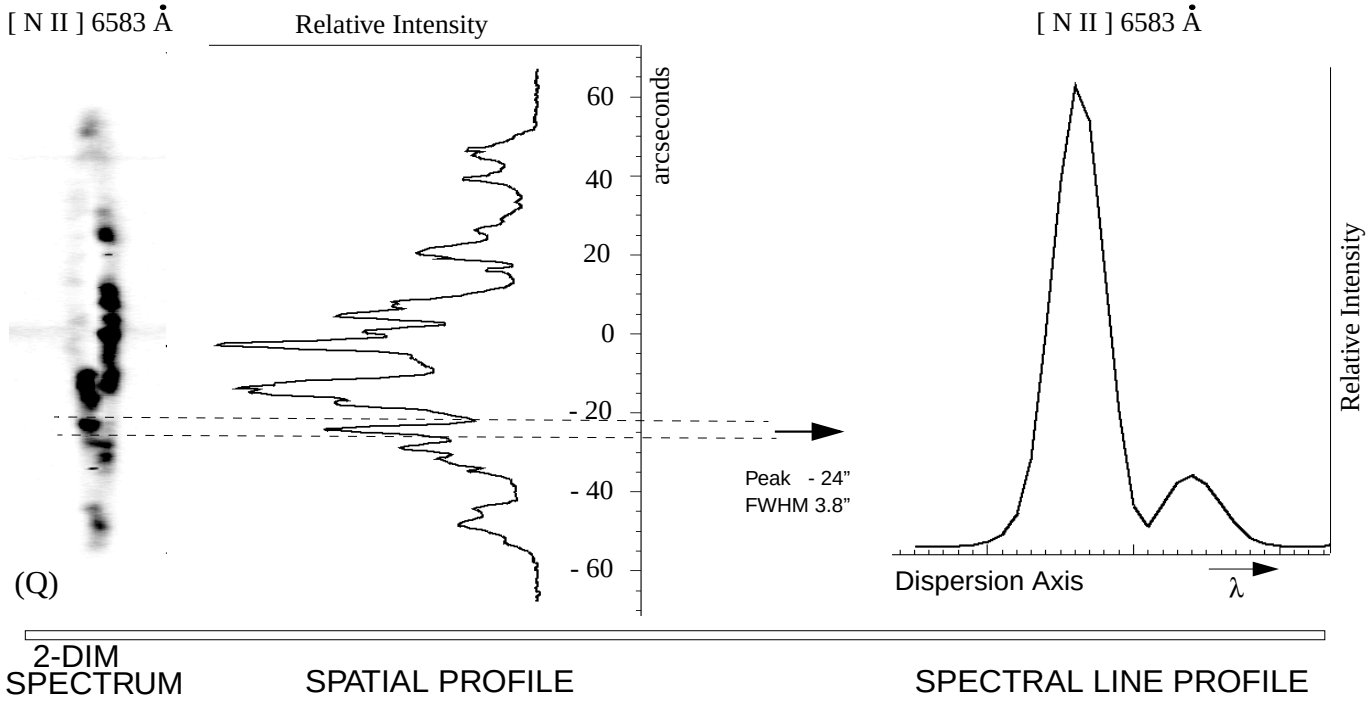

Fig. 4. Schematic diagram of the procedure we followed to identify and to select the clumps within each line profile, to determine their location and spatial extent, and to extract the one-dimentional spectra.

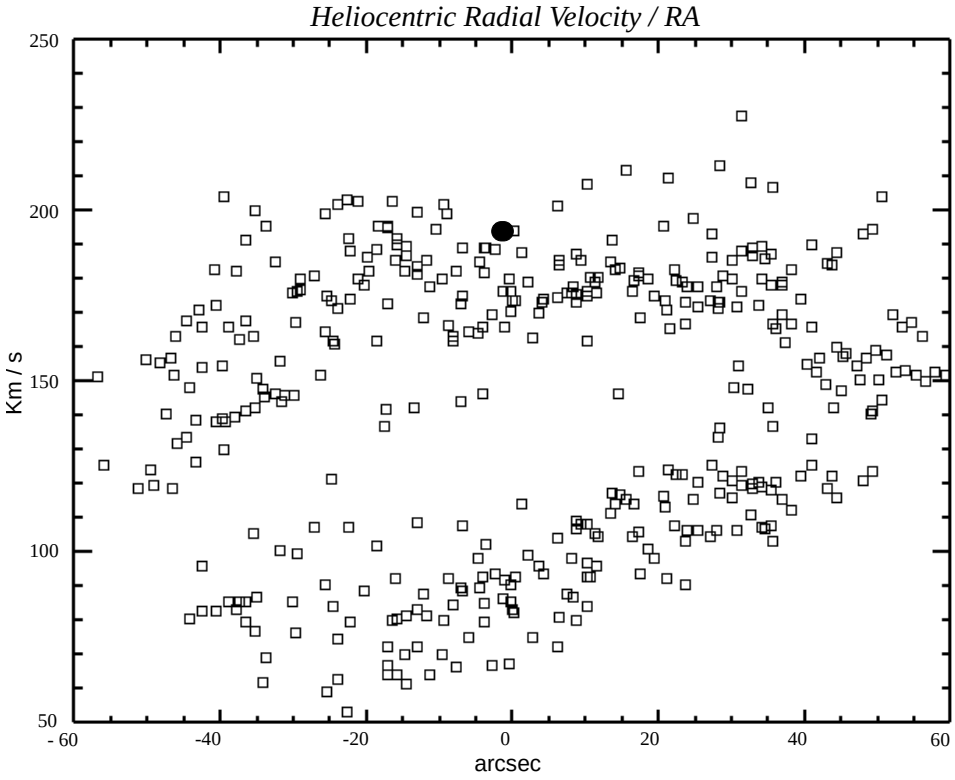

Fig. 5. The heliocentric radial velocity map of the nebula, derived from the [NII] λ 6584 line profile, is here plotted as a function of position with respect to the star. The black dot marks the position of the central star WR 124.

these two structures coexist in the circumstellar environment of WR 124. This is both a revision and an improvement over the conclusions reached by Nota et al. (1995a) where, given the lower resolution of the data, only the bipolar outflow was detected.

If we assume a distance of 4.5 Kpc (Pişmiş & Recillas-Cruz 1979), we can estimate dynamical timescales of 2.1×10^4 yrs and 1.2×10^4 yrs for the shell and the bipolar outflow, respectively.

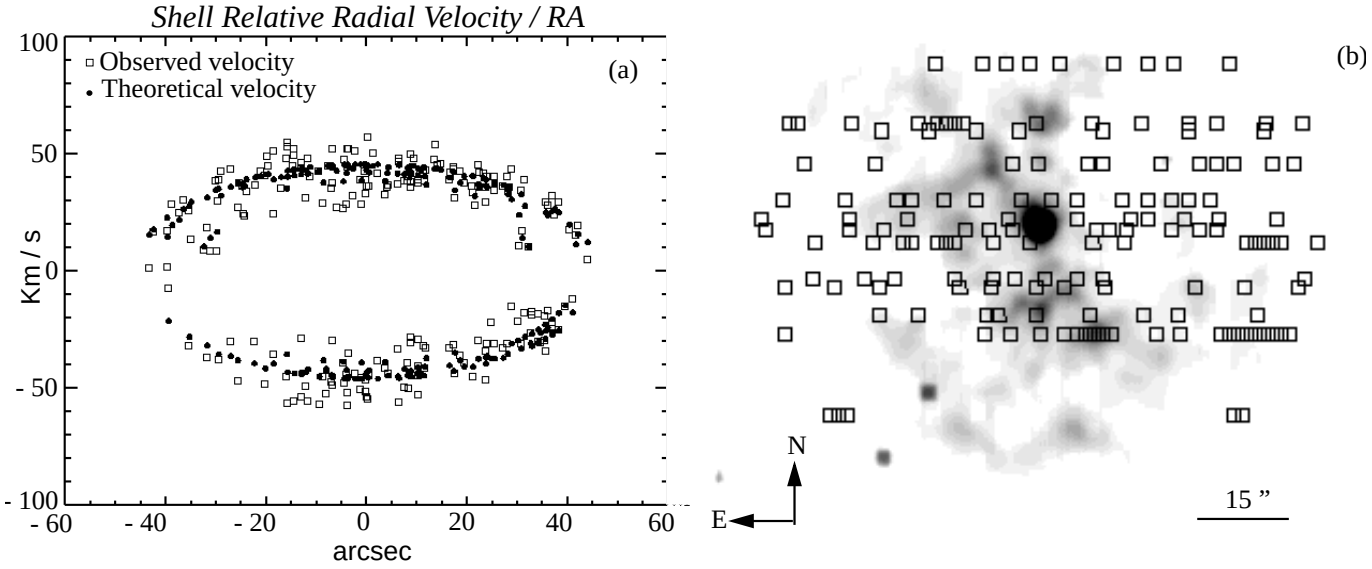

Fig. 6a and b Composite representation of the radial velocity map (left panel) and of the spatial distribution (right panel) of the points belonging to the expanding shell, superimposed to a large field image of M 1-67 The left panel shows the velocity distribution (filled dots) modelled for a shell 46″ in radius expanding with a velocity of 46 km s^{-1}, to be compared with the data (empty squares).

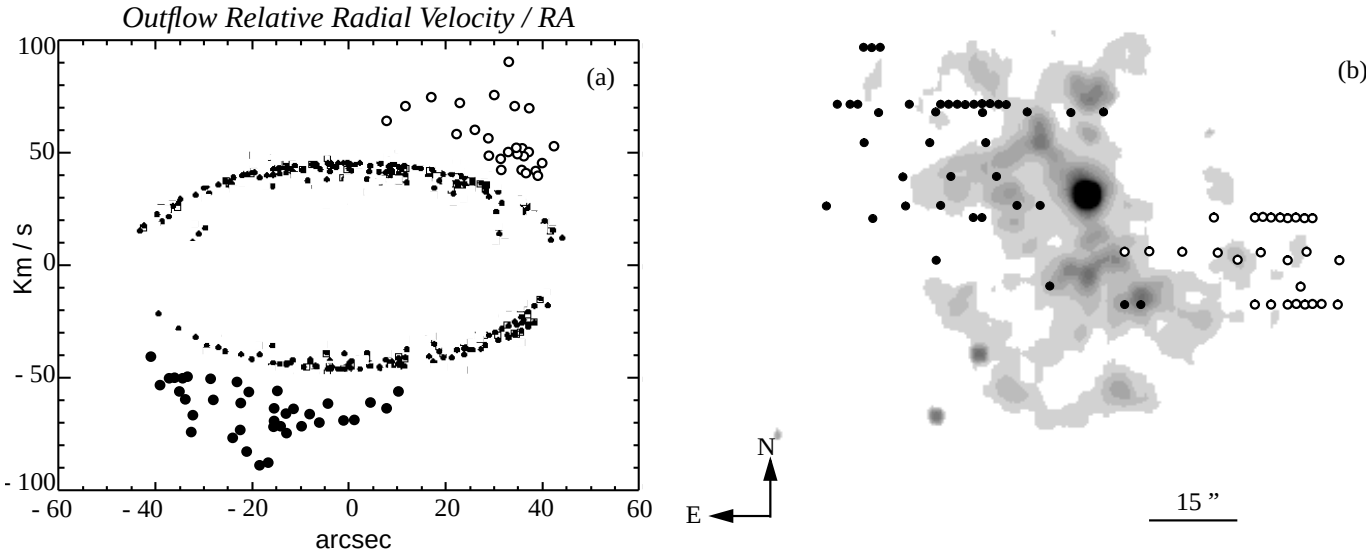

Fig. 7a and b Composite representation of the radial velocity map (left panel) and of the spatial distribution (right panel) of the points belonging to the bipolar outflow, superimposed to a large field image of M 1-67.

Pişmiş & Recillas-Cruz (1979) had first suggested a model based on an anisotropic outflow to explain their kinematical observations of M 1-67. However, Chu & Treffers (1981) were the first to notice the contemporaneous presence of two distinct motions in the circumstellar environment of WR 124: a narrow component, concentrated near the central star, and a second broader component, covering a much larger extension. Chu & Treffers had estimated two dynamical timescales, in the range 10^4 to 10^5 yr. These values were calculated assuming a distance of 2 Kpc so the absolute timescales would need to be here revised in order to be compared with our findings. However, the broader component resulted to be older than the narrow component detected close to the star. Chu & Treffers did not attempt to resolve spatially the two components. Within the uncertainties associated with their, and our data, it seems plausible to assume that their older component is the spherically expanding shell, while the second, younger component detected closer to the star would be the bipolar outflow.

Of all published kinematical studies, SC definitely had the highest spectral resolution, and in principle we would have expected them to detect the bipolar outflow, while they only found the expanding shell. As already mentioned in Nota et al.(1995a) we believe this is due to the coarse spatial coverage of their spectroscopic observations, which unfortunately missed most of the clumps in the spatial regions associated with the outflow.

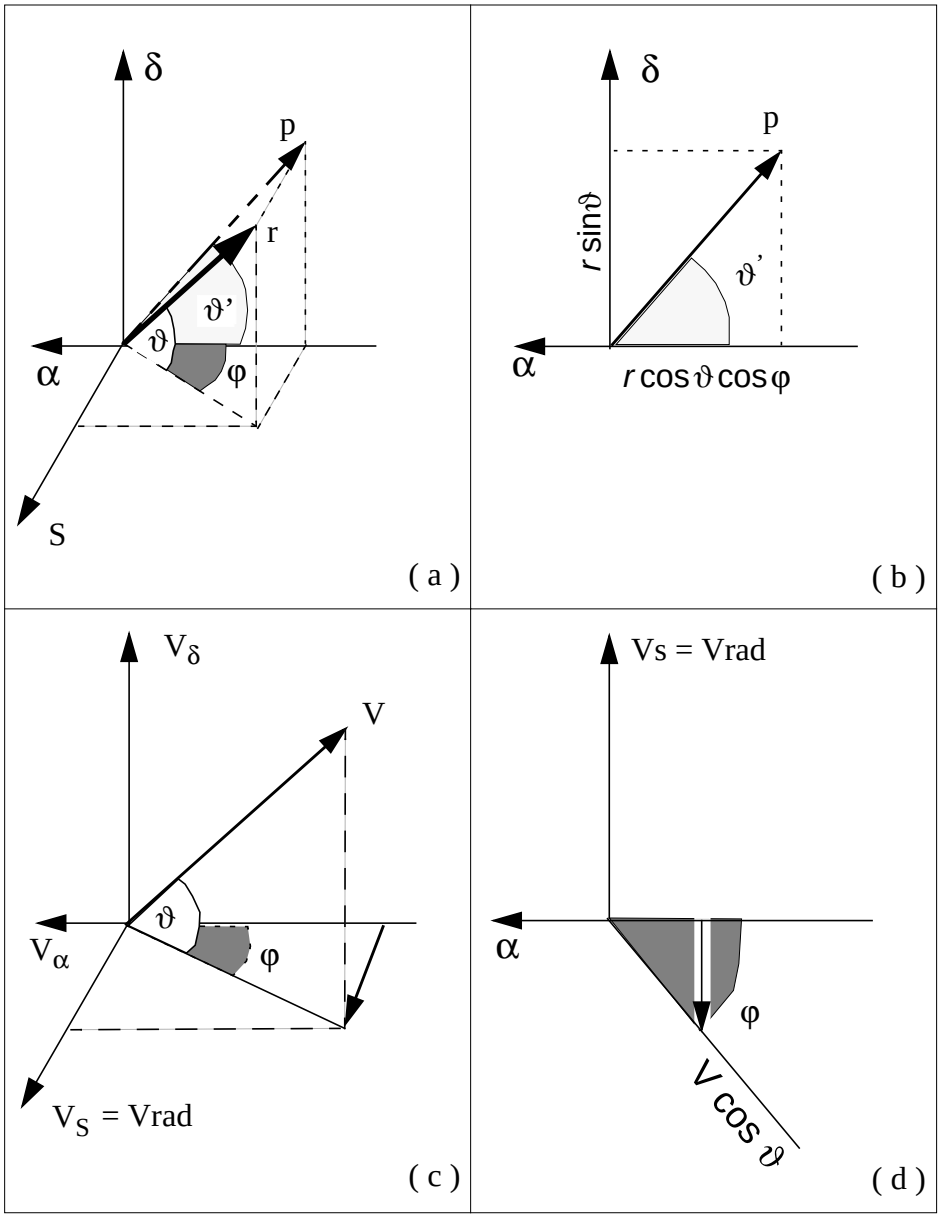

Fig. 8a–d The coordinate system we have adopted to describe the orientation of the nebula in the sky is here shown in panel **a**. α, δ identify the plane of the sky, S is the line of sight. Panel **b** defines the projected orientation of the bipolar outflow on the plane of the sky. Panels **c** and **d** define how we use the radial velocity information to derive the *true* orientation of the outflow in the sky. V_α and V_δ are the components of motion along right ascension and declination, V_S is the radial velocity we measure.

It is plausible that both structures we detect have originated during the post main-sequence evolution of the central star, most likely during two subsequent outbursts in a LBV phase. The fact that the M 1-67 nebula is composed of ejected material had already been established by SC on the basis of dynamical considerations (the high peculiar velocity shared by both the star and the nebula). In addition, Esteban et al. (1991) found that the nebula has a N enhancement and O deficiency which is typical of stellar processed material. Esteban et al. (1991) measured densities of 10^3 cm^{-3} in the central parts, but five times lower in the outer regions. From our data, we could estimate the electron density from the [SII] $\lambda\lambda$ 6717/6731 ratio across the nebula. More precisely, we measured such ratio in correspondence to all the positions of the nebula for which we have radial velocities. By excluding those structures characterised by a low S/N ($<$ 3) for which it was not possible to accurately measure the [SII] ratio, we obtained a sample of $\simeq$ 270 density values, uniformly distributed over the entire nebula.

We derived the electron temperature only for the slit position M, for which we obtained a spectrum in the range 5080 - 6025 Å. Because of the low S/N ratio of the data, we integrated the spectrum over the entire spatial extension of the slit and obtained a dereddened [NII]$\lambda\lambda$ (6548+6583)/5755 ratio of 455. At the same slit position, we measured a mean density of 940 cm^{-3}, and therefore calculated an electronic temperature T_e = 5900 $\pm$ 400 ^{o} K, which is in very good agreement with the average value of 6200^{o}K obtained by Esteban et al. (1991).

We adopted our derived electronic temperature value of 5900^o K and calculated the electron density for the 270 positions. We find that the density can be as low as 150 cm^{-3} in the outer nebular regions but grows up to 2400 cm^{-3} towards the center of the nebula. In Fig. 9, we have plotted the electron

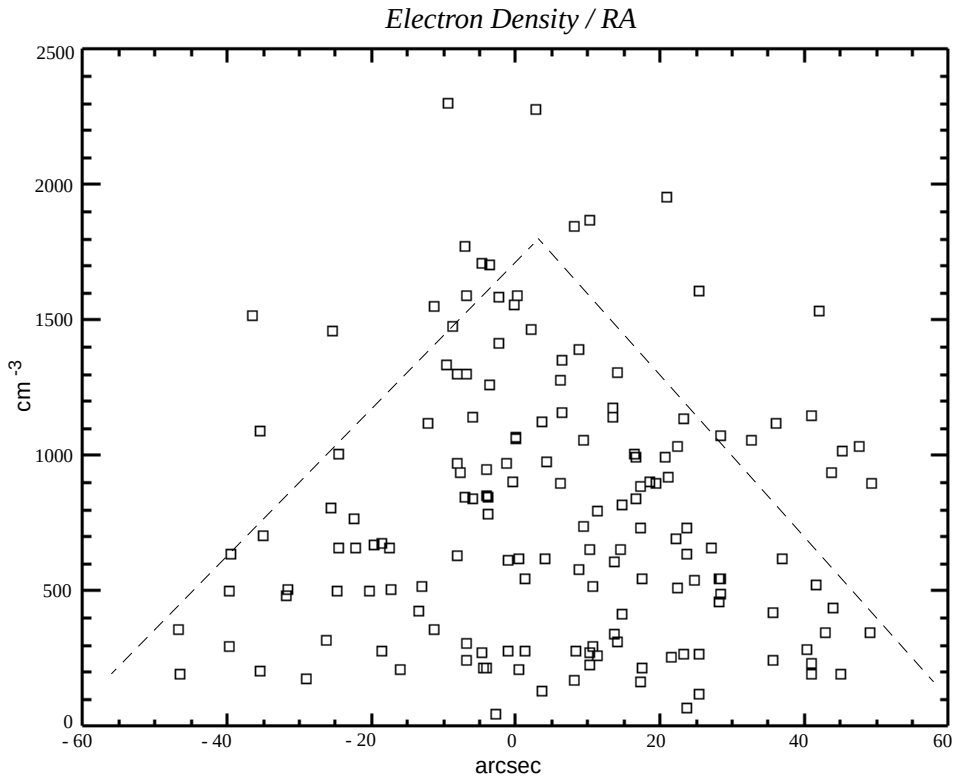

Fig. 9. Electron density distribution *vs* as a function of position with respect to the star, along the α axis.

densities as a function of position with respect to the star: the trend of increasing electronic density approaching the center of the nebula is unambiguous. Our findings are in very good agreement, but even more extreme, than the previous investigations (SC and Esteban et al. 1991) who obtained values ranging between 200 cm^{-3} for the outer zones and 1000 $\pm$300 cm^{-3} for the central region. We do not detect any significant difference in density between the two motion components.

Esteban et al. (1991) found that the oxygen abundance is homogeneous and very low across the nebula: they derived an oxygen depletion by a factor 5 to 7.5 with respect to a typical HII region. The ratio N/H was found to be 4 to 7 times higher than expected, and N/O = 3.0 in number due to the oxygen underabundance. By comparing their derived abundances with the model predictions for surface abundances by Maeder (1990), Esteban et al. (1991) found that the nebular abundances correspond to initial masses of 25-40 $M_\odot$ at a point near the end of the RSG phase. On the other hand, other observational data point to an LBV progenitor for this nebula: the mass of ionized gas is quite small, only 0.8 $M_\odot$ (SC), and the radius of 0.9 pc is also quite small to be associated with a RSG phase (Smith, 1996). In addition, the nebular expansion velocities (40-100 km s^{-1}) are somewhat higher than what we would expect in a RSG ejected nebula, which typically would be in the range 10-20 km s^{-1}.

Unfortunately with the present data it is not possible to carry out a thorough chemical analysis of the nebular abundances in the clumps, which would establish whether there are composition differences in the material ejected during the two phases. Such a finding could probably assess whether mixing has occurred in the outer star layers, possibly due to rotation.

It is interesting to notice that the presence of a bipolar outflow enhances the similarity of the M 1-67 nebula with other LBV nebulae, which almost all display some degree of bipolarity (Nota et al. 1995b). It is not clear, at this point, what physical mechanism has produced such different morphologies (an expanding shell and a bipolar outflow) in such a relatively short time.

Multiple shells are not uncommon among LBV nebulae: high resolution HST [NII] images of the AG Carinae nebula (Nota et al. 1996c) show two nested, concentric shells, which display differences in their expansion velocities. Two distinct nebulae have been detected in the circumstellar environment of P Cygni (Barlow et al. 1994; Meaburn et al. 1996): an inner nebula, 22″ in diameter, probably ejected $\simeq$ 900 yrs ago, and an outer nebula, 1.6′ in size, $\simeq$ 1100 yrs older.

From a theoretical point of view, multiple outbursts are expected in LBVs: both Langer et al.'s (1994) evolutionary scenario, where enhanced mass loss keeps the star on the blue side of the Eddington-instability limit in the HRD, and Stothers & Chin's (1996) model, where the major mass loss occurs in a single ejection event during a brief red supergiant phase (RSG), foresee, after the main outburst which generates the nebula, a number of subsequent outbursts of minor intensity. At every ejection, a decreasing amount of mass would be lost. It is likely that the ejected layers would not thoroughly mix, and that the nebulae we presently observe would be the accumulation of the subsequent outbursts.

More puzzling is the coexistence of a spherical shell and a bipolar outflow, although this phenomenon has also been observed in some PN. In the case of NGC7027, for example (Bond

et al. 1997), there is evidence that the very early ejection is quite spherically symmetric, while an axially symmetric nebula has been produced at later stages.

An explanation currently proposed to explain the PN observations (Livio 1997) invokes a binary scenario in a *common envelope (CE)* phase. The core of the AGB star and of the secondary star spiral in, engulfed by a common, extended, envelope, eventually leading to the ejection of the envelope itself. Hydrodynamical simulations of the CE phase have shown that in the early stages the ejection is quite spherically symmetric. At the end of this dynamical phase, a thick disk is corotating with the binary, and orbital decay continues through the viscous interaction of the thick disk with the envelope. The matter ejected in these later phases is predominantly concentrated around the orbital plane, producing a noticeable density contrast in the nebula, and the appearance of a bipolar symmetry.

Applied to LBVs and related objects, the question of binarity has been long standing and unresolved, mainly due to the observational difficulties of observing close binaries in these very massive systems. Further dedicated observations are needed to establish whether LBVs are indeed binary systems. In the special case of M 1-67 higher resolution images (HST) would also greatly improve the study of the spatial distribution of the two motion components and to place more accurate limits to their orientation and extent, especially in the region very close to the star where the bipolar outflow seems to originate.

Acknowledgements. AP acknowledges partial support from the STScI DDRF throughout the duration of the work. The authors wish to thank Mario Livio, Linda Smith, Norbert Langer and Guillermo García-Segura for many useful discussions on the subject.

References

Barker, T. 1978, ApJ, 219, 914
Bertola, F. 1964, PASP, 76, 241
Bond, H.E., Ciardullo, R., Fullton, L.K. & Schaefer, K.G. 1997, in preparation
Chu, Y.-H. & Treffers, R.R. 1981, AJ, 249, 586
Clampin, M., Golimowski, D. & Durrance, S. 1991, in Active and Adaptive Optical System, ed. M. Ealey (Proc. SPIE, 1542), 165
Cohen, M. & Barlow, M.J. 1975, ApJ, 16, L165
Crawford, I.A. & Barlow, M.J. 1991, A&A, 249, 518
Cudworth, K.M. 1974, AJ, 79, 1384
Esteban, C., Vìlchez, J.M., Smith, L.J. & Manchado, A. 1991, A&A, 244, 205
Esteban, C., Smith, L.J., Vìlchez, J.M. & Clegg, R.E.S. 1993, A&A, 272, 299
Kohoutek, L. 1978, IAU Symp. 76, 47
Langer, N., Hamann, W.-R., Lennon, M., Najarro, F., Pauldrach, A.W.A. & Puls, J. 1994, A&A, 290, 819
Livio, M. 1995, in Asymmetrical Planetary Nebulae, ed. A. Harpaz & N. Soker(Bristol: IOP), p. 51
Livio, M. 1997, Space Sci. Rev., in press
Meaburn, J., Lopez, J.A., Barlow, M.J., Drew, J.E. 1996, MNRAS, 283, 69
Merrill, P.W. 1938, PASP, 50, 350
Nota, A., Clampin, M., Sirianni, M., Greenfield, P., Golimowski, D.A. 1995a, IAU Symp. 163, 78
Nota, A., Livio, M., Clampin, M. & Schulte-Ladbeck, R. 1995b, ApJ, 448, 788
Nota, A., Clampin, M., García-Segura, G., Leitherer, C., Langer, N., 1996, in Science with the Hubble Space Telescope II, ed. P. Benvenuti, F.D. Macchetto, & E. J. Schreier (STScI - ECF), p. 398
Perek, L., Kohouthek, L. 1967, Catalog of Galactic Planetary Nebulae, Prague, Czechoslovak Institute of Science
Pişmiş, P. & Recillas-Cruz, E. 1979, Rev. Mexicana Astr. & Astrophys., 4, 271
Sharpless, S. 1959, ApJS, 4, 257
Smith, L.J. 1996, in Wolf-Rayet Stars in the Framework of Stellar Evolution, ed. J.M. Vreux, A. Detal, D. Fraipoint-Caro, E. Gosset, G. Rauw, (Liege: Institut d'Astrophysique), p.381.
Solf, J. & Carsenty, U. 1982, A&A, 116, 54, (SC)
Stothers, R.B. & Chin, C.-w., 1996, ApJ, 468, 842
van der Hucht, K.A., Jurriens, T.A., Olnon, F.M. et al. 1985, A&A, 145, L13